Bulletin of the Seismological Society of America. Vol. 66, No. 1, pp. 125–151. February 1976

THE IDENTIFICATION OF BUILDING STRUCTURAL SYSTEMS I. THE LINEAR CASE

BY FIRDAUS E. UDWADIA AND PANOS Z. MARMARELIS

ABSTRACT

This paper investigates the response of structural systems to strong earthquake ground shaking by utilizing some concepts of system identification. After setting up a suitable system model, the Weiner technique of nonparametric identification has been introduced and its experimental applicability studied. The sources of error have been looked into and several new results have been presented on accuracy calculations stemming from the various assumptions in the Wiener technique.

The method has been applied in studying the response of a 9-story reinforced concrete structure to earthquake excitation as well as ambient vibration testing. The linear contribution to the total roof response during strong ground shaking has been identified, and it is shown that a marked nonlinear behavior is exhibited by the structure during the strong-motion portion of the excitation.

INTRODUCTION

The development of design procedures for the aseismic design of structures necessitates the ability to determine structural responses to large ground excitations. To do this, one requires a proper understanding of the system through a quantitative identification of the actual physical process. Recent studies on the observed response of structures to strong ground shaking indicate marked nonlinearities in system dynamics (Udwadia and Trifunac, 1972). Response calculations of structural systems to large earthquake excitations would therefore necessarily involve a proper inclusion of these nonlinear features. The identification problem would then be one of defining the dynamics of the complete nonlinear system.

In its most general interpretation, knowledge of the dynamic characteristics of a structure implies cognizance of the functional relations between the excitations and the responses at various points of the structure. Such an identification is ultimately aimed at obtaining a mathematical representation, or model, of the system. Having obtained by some means such a mathematical model, the investigator can then simulate the system response to any input. The usefulness of such a model would lie in the feature that structural responses to large ground motions can then be computed. Full-scale vibration tests fall short of such a capability due to the inability to produce large well-controlled inputs.

The problem of identifying a structural system may be formulated from two broad viewpoints. In the first, the mathematical structure of the model is given or assumed, but its parameters are not. In the second, no *a priori* information whatsoever is specified regarding the structure of the model. In the present paper, attention is focused on the second of these viewpoints.

Most of the work done so far in the area of system identification as applied to structural systems has been viewed from the parameter estimation approach (Nielsen, 1966; Gersch *et al.*, 1972; Iemura and Jennings, 1973), where the system model is assumed to be known. Moreover, such analyses have generally assumed linear system models. Although structural systems subjected to strong ground shaking are almost universally

nonlinear in nature, there have been no previously reported attempts to characterize the dynamics of such systems through the application of a general theory of nonlinear systems. This can be readily understood because the theory developed by Wiener was not available prior to about 1950 and also because it was particularly obscure to the non-mathematician.

Part I of this study presents the general structural identification problem. It briefly outlines the basic Wiener theory (Wiener, 1958) of nonlinear system characterization, so as to provide the necessary background for an understanding of its extent of applicability to building structural systems using earthquake and microtremor ground-motion inputs. The advantages of such a technique together with its encumbent shortcomings are pointed out and methods of improvement suggested. Input-output data obtained from a nine-story reinforced concrete structure during the 1971 San Fernando, California, earthquake are analyzed according to these procedures. Together with the two components (NS and EW) of strong ground shaking considered, data in the EW direction from an ambient test are also studied. In this part, the linear characterizations of the building (in the two directions) are obtained and discussed. The effects of possible error sources and the possible effect of the nonlinearities in adversely affecting the linear characterizations of the system are analyzed.

Part II concentrates on the nonlinear behavior of the same structure as obtained through the determination of the higher-order system kernels and introduces the nonlinear feedback model. The effect of various error sources in the computation of the nonlinear kernel is discussed. Model responses for the same inputs are determined using first, the linear characterizations and then, the nonlinear characterizations.

The studies indicate that structures subjected to strong ground shaking could portray strong nonlinear effects. The nonlinear models synthesized using Wiener's technique show that marked improvements in the response prediction are effected by the inclusion of the nonlinear features.

The Structural Identification Problem

In general, the system identification problem may be characterized by three different sets of considerations: a class of models, M, a class of inputs, I, and an error criterion, ε. It usually takes the following form: Given the system response for the class of inputs I, identify a member from the class of models, M, which minimizes some error criterion, ε. This error criterion, ε, usually takes the form of a norm of the difference between the system performance and the model response. These three features of the identification problem are not independent of each other, but would influence each other considerably. A common example is the use of a model from the class of linear systems for the analysis of structural responses to low-level excitations (inputs) such as microtremors or wind.

System models may be broadly classified as parametric and nonparametric models:

(*a*) *Parametric models.* Here the configuration and mathematical description of the system to be identified are assumed to be known, and the several parameters on which the system response is assumed to depend are estimated. The formulation of the identification task eventually becomes a search in "parameter" space which attempts to minimize a suitable error criterion. Although such a problem formulation is useful, in many instances it suffers from certain defects in terms of the three basic quantities in system identification mentioned above.

(*b*) *Nonparametric models.* The structural configuration of the system is considered unknown (no assumptions are made about it). In this case identification becomes a search in "function" space, i.e., a class of functionals within a wide class of systems.

Approach (*a*) has several inherent disadvantages, as well as advantages. It requires some *a priori* assumptions regarding the nature of the system. Then a search is made for the best model within this parameter space described by the assumed state equations. Such models could lead to large errors in complex structures, in the case of a linear system representation, if the order of the mathematical model does not coincide with the order of the actual structure. This could be an important difficulty in large structures where the mass and stiffness distributions are not properly understood so as to obtain an accurate enough representation of the model order. Nonparametric representations do not require the order of the system to be explicitly known. The identification of such a parametric model becomes even more difficult if the system is nonlinear. In this case, the search in parameter space may become both difficult and costly in computer time.

The use of any one modeling approach will ultimately depend upon the purpose of the identification and the amount of *a priori* information we have on the system functional. To a large extent, the nonparametric approach encompasses the parametric approach; for after the system functional is determined, the system parameters can be easily identified from this functional. A combination of the two approaches would then seem fruitful, the nonparametric approach forming a logical prelude to parameter estimation. Furthermore, if the aim is to study the time response and to be capable of predicting it for a given class of inputs, the nonparametric approach is ideal.

In this paper we have taken the nonparametric viewpoint, i.e., our ultimate aim of the identification process is to predict the response rather than to estimate various parameters. A characteristic feature of such a general approach is that in our attempt to predict the time history of the response of the structure, which we look upon as a black box unrestrained by any *a priori* assumption about the system, we lose some physical understanding of the various details within the black box. We obtain an overall picture of the complete structure in terms of certain functions rather than in terms of the more physically understandable assumed model parameters.

The feedback model

The input-output "black-box" model of a structure which is subjected to an input, x, measured at the basement, and whose response, y, is measured at the roof, is shown in Figure 1a. Figure 1b shows a simplified model of the soil-structure system schematically. Typically, we shall be interested in the basement record, $x(t)$, and the roof record, $y(t)$. The true input, i_t, to the system passes through the structure, represented by the black box, B, reaches the top of the structure, and is reflected back by means of the element R. The signal then descends through the structure depicted by the element B^*. On reaching the foundation, a part of the signal gets reflected back into the structure. The part which does this can be imagined as being produced by the signal j going through the black box L. Also, a part of the signal (which can similarly be imagined as produced by the signal j going through the element T) is transmitted to the ground. This transmitted signal is further modified as it passes through the ground (element G). Finally, the signal interferes with the incoming signal, i_t, completing the "feedback loop."

Each of the black boxes shown in Figure 1 indicate nonlinear, time-variant, finite memory subsystems. Since the signal speeds in structural systems are relatively small (in comparison with characteristic response times), each of the boxes shown would generate time-delayed outputs. One could visualize this by imagining that each black box is composed of two elements: a time-delay element, which simply delays the signal, and a filter element, which alters this delayed signal, allowing it to pass through with infinite signal speed. The feedback mechanism makes such time delays critical in the

response analysis. Furthermore, it must be noted that the delay created by the delay element of any one black box may be quite comparable to the characteristic time of the filter element it contains.

A simpler visualization of the system can be made by lumping all the elements in the

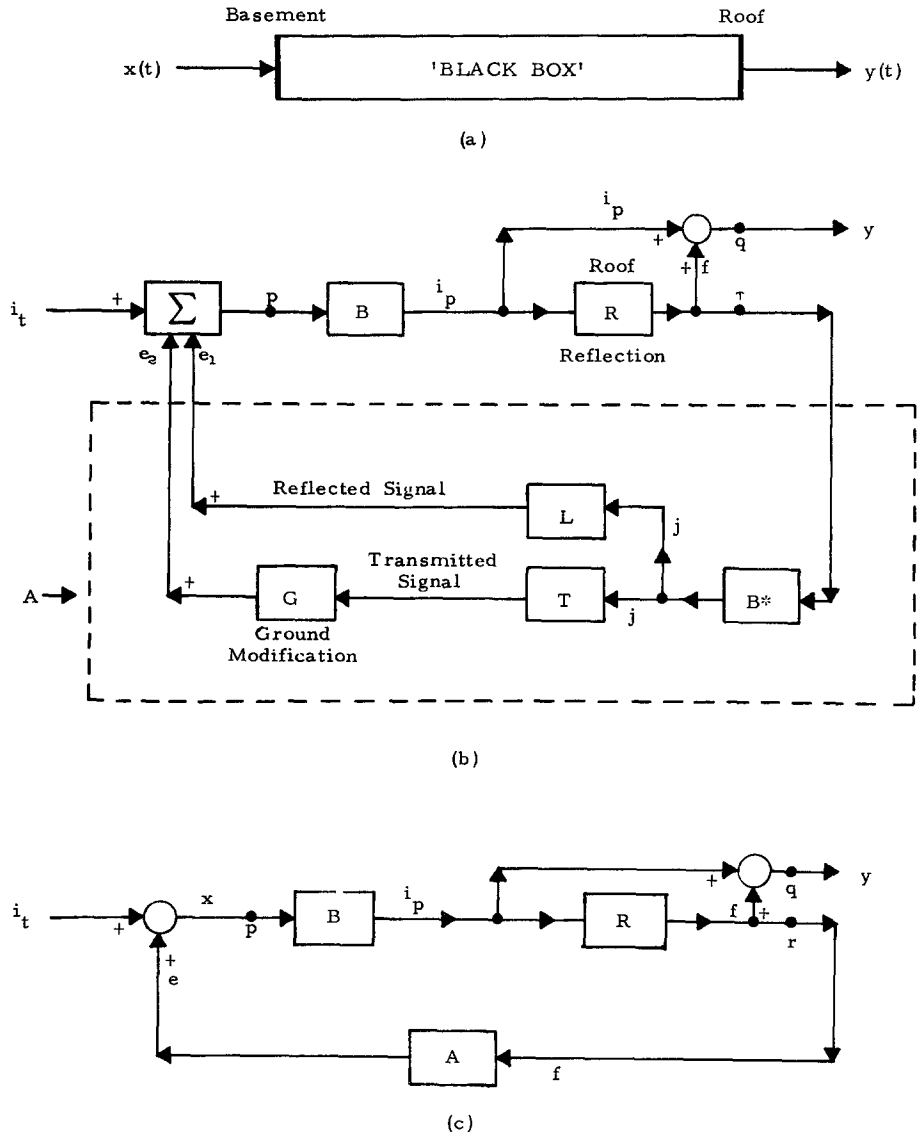

FIG. 1. (a) Black box model of structural system; (b) idealized feedback model for soil structure systems; (c) analysis of structural system S from input-output data between node points p and q.

feedback loop into only one element, designated by A. The characterization depicted in Figure 1c then emerges. The input (x)-output (y) relation essentially observes the black boxes B and R between the node points p and q (Figure 1c). In this paper the properties of these black boxes shall be studied from an analysis of the p-q segment of the visualized structural model.

The effect of feedback, which shall not be considered in detail in this paper, can be qualitatively looked upon for the sake of illustration as follows: Assuming for simplicity that all the elements are linear,

$$\tilde{\imath}_p = B\tilde{x} \tag{1}$$

$$\tilde{f} = R\tilde{\imath}_p \tag{2}$$

and

$$\tilde{y} = \tilde{\imath}_p + \tilde{f} \tag{3}$$

where the tildes represent Laplace transforms and the capital letters represent transfer functions. Also,

$$\begin{aligned}\tilde{e} = \tilde{e}_1 + \tilde{e}_2 &= B^*(L+GT)\tilde{f} \\ &= A\tilde{f} = RAB\tilde{x}\end{aligned}$$

where

$$A = B^*(L+GT)$$

and

$$\tilde{x} = \tilde{\imath}_t + \tilde{e},$$

thus yielding

$$\tilde{y} = \frac{B+RB}{1-RAB}\tilde{\imath}_t. \tag{4}$$

Assuming that our measurement is at the roof, $R \approx 1$ so that

$$\tilde{y} \approx \frac{2B}{1-AB}\tilde{\imath}_t.$$

If there is no feedback, $e = 0$ and $i_t = x$. In that case

$$\tilde{y} = \tilde{\imath}_t \cdot (B+RB) = S\tilde{\imath}_t.$$

From equation (4) it may be seen that large output amplitudes will be obtained at frequencies (1) which correspond to the poles of B with $AB \to 0$, and (2) which correspond to the zeros of the function $(1-RAB)$.

The above discussion, although crude in its assumptions, heuristically serves to show that large outputs, y, can be obtained at the frequencies that not only coincide with the poles of B but also with those that may correspond to the zeros of $(1-RAB)$. Thus, keeping in mind that the output, y, can be largely influenced by the feedback, e, let us proceed to the analysis of the p-q segment of the system by considering the response of the system to microtremor and earthquake ground motions.

System stationarity

An important decision that has to be made before the identification of a process is undertaken is the time length of record that one needs to utilize to obtain reliable information on the system. This in turn is strongly dependent on the nature of the system being studied. In general, for time-invariant systems, the identification is improved by the use of longer record lengths due to the effect of input-output noise smoothing as well as parameter smoothing (Marmarelis and Naka, 1973, 1974). However, for time-variant systems the length of record chosen must be sufficiently long so as to ensure adequate noise and parameter smoothing, and yet be sufficiently short so that the system properties do not change appreciably during the time length required to complete the identification.

Under low levels of excitation, such as wind and microtremors, structural systems are primarily excited in the linear range and usually do not undergo any perceptible deteriora-

tion, so that they could be considered stationary and the problem taken to be one of the "time-invariant" type. Under large dynamic loads, however, structural systems show nonlinear responses (Iemura and Jennings, 1973) and often exhibit a deteriorating behavior, so that even during the measurement interval the characteristics of the system may not remain invariant with time. To study the earthquake response of a structure, then, it is necessary that the structural model should include nonlinear time-variant features in it.

Since the general nonlinear identification of time-variant systems is beyond the scope of this study, we shall assume that the structural characteristics of a system remain invariant over the time length during which the identification is carried out. As described in the section on experimental applicability, a general idea about the time length over which severe structural changes do not occur can be obtained through techniques such as moving-window analysis or sequential filtering (Udwadia and Trifunac, 1975).

THEORY

Wiener's major contribution to the general theory of nonlinear system identification was the use of white noise as the input test signal. White noise is a random signal which contains all frequencies with equal energy, and, therefore, it can serve to test the system exhaustively. This is because any input function over a finite interval can be approximated arbitrarily closely by some segment of a Gaussian white-noise signal (i.e., a white-noise signal whose amplitude has a Gaussian distribution). In practice, of course, the test white-noise input is band-limited (i.e., it cannot contain frequencies which are arbitrarily high) and it is finite in duration. However, the same arguments are valid provided that (a) the bandwidth of the white-noise signal completely covers the bandwidth of the system under testing and (b) the duration of the white-noise test signal is sufficiently long in comparison with the characteristic times of the system. The resulting characterization, using these methods, is a *statistical average characterization*, and two systems which respond identically to Gaussian white noise would then be considered equivalent.

For a causal (physical) system S, whose input is $x(t)$ and output is $y(t)$, we have

$$y(t) = F[t; x(\tau), \tau \leqq t] \tag{5}$$

where F is a functional whose value (a real number) at time t depends only on the past values of the input. For a time-invariant system with finite memory, M, equation (5) reduces to

$$y(t) = F[x(\tau), t-M \leqq \tau \leqq t]. \tag{6}$$

The "memory" of a system is approximately equivalent to the "settling time" of the system.

Volterra showed that equation (6) can be written as

$$\begin{aligned} y(t) = {} & g_0 + \int_0^\infty g_1(\tau)x(t-\tau)d\tau + \iint_0^\infty g_2(\tau_1, \tau_2)x(t-\tau_1)x(t-\tau_2)d\tau_1 d\tau_2 \\ & + \iiint_0^\infty g_3(\tau_1, \tau_2, \tau_3)x(t-\tau_1)x(t-\tau_2)x(t-\tau_3)d\tau_1 d\tau_2 d\tau_3 + \ldots \end{aligned} \tag{7}$$

where $g_i(\tau_1, \tau_2, \ldots, \tau_i)$ is a symmetric function of its arguments. The set of $\{g_i\}$ is called the set of Volterra Kernels of the system. This set of kernels completely characterizes the dynamic response of a nonlinear, time-invariant system with finite memory (Brilliant, 1958). Wiener (1958) has shown that equation (7) can be written as an infinite series

$$y(t) = \sum_{n=0}^{\infty} G_n[h_n, x(t)] \tag{8}$$

where $\{G_n\}$ form a complete set of orthogonal functionals with respect to a Gaussian

white-noise input $x(t)$. The system would be completely characterized if the kernels $\{h_n\}$ are all determined. The orthogonal property of functionals is expressed as

$$E\{G_n[h_n, x(t)]G_m[h_m, x(t)]\} = 0, \text{ for } m \neq n$$
$$= \text{constant, for } m = n \tag{9}$$

where $E\{\cdot\}$ denotes the expected value of the quantity in the brackets. Moreover, the Wiener G-functional of degree n is such that it is orthogonal to all functionals of degree less than n.

The first four functionals of this series are

$$\begin{aligned}
G_0[h_0, x(t)] &= h_0 \\
G_1[h_1, x(t)] &= \int_0^\infty h_1(\tau)x(t-\tau)d\tau \\
G_2[h_2, x(t)] &= \iint_0^\infty h_2(\tau_1, \tau_2)x(t-\tau_1)x(t-\tau_2)d\tau_1 d\tau_2 \\
&\quad -P\int_0^\infty h_2(\tau_2, \tau_2)d\tau_2 \\
G_3[h_3, x(t)] &= \iiint_0^\infty h_3(\tau_1, \tau_2, \tau_3)x(t-\tau_1)x(t-\tau_2)x(t-\tau_3)\cdot \\
&\quad \cdot d\tau_1 d\tau_2 d\tau_3 - 3P\iint_0^\infty h_3(\tau_1, \tau_2, \tau_3)x(t-\tau_1)d\tau_1 d\tau_2
\end{aligned} \tag{10}$$

where P is the spectral density level of the input white noise, i.e., $P = \phi_{xx}(f)$ is the power spectrum of $x(t)$ at frequency, f. The set of symmetric kernels $\{h_n\}$ characterizes the system and could be thought of as being generalized "impulse responses" of the nonlinear system. The first order kernel $h_1(\tau)$ corresponds to the impulse response function of linear systems theory. The nonlinear kernels describe quantitatively the nonlinear cross talk between various portions of the past input as it affects the present response. For example, for a second-order nonlinear system, i.e., a nonlinear system for which $h_k = 0$ for $k \geqq 3$, $h_2(t, t-t_\alpha)$ indicates the deviation from linear superposition that arises in the response at a time $t \geqq t_\alpha$ when the inputs comprise two delta functions, one at time $t = 0$ and the other at time $t = t_\alpha$ (cf., part II of this study). The kernels may thus be interpreted so as to reveal interesting physical properties of the system dynamics.

In Wiener's formulation of the method a general nonlinear memory system was represented by the cascade combination of a linear system with multiple outputs and a nonlinear no-memory system. This was accomplished by expanding the past of the system input in terms of Laguerre polynomials (a linear transformation) and then expanding the system functional defined on the Laguerre coefficients in terms of Hermite functions (a nonlinear no-memory process since it involves multiplication of the terms of the Hermite expansion). Thus, the identification problem was reduced to determining the coefficients of this expansion (Bose, 1956).

The Laguerre polynomial expansion was chosen basically because it could be accomplished easily by linear analog computation. The Hermite functions were picked by Wiener to expand the system functional because they have some convenient properties with respect to Gaussian white-noise signals.

However, this formulation is impractical and difficult to apply in an experimental situation for the following reasons:

1. The number of coefficients needed to characterize almost any system, linear or nonlinear, is extremely large. If n coefficients are used in the Laguerre expansion to describe the past of the input at any time and p coefficients are used to expand the system functional in terms of Hermite functions, then the number of coefficients needed to characterize the system is p^n. Exploratory calculations showed that, even for a simple

nonlinear system such as a system with only a second-order nonlinearity, the number of characterizing coefficients has to be as large as 10^{10}.

2. The computing time required for the evaluation of the characterizing coefficients is extremely long, especially since the computation has to be performed serially. In the synthesis phase, when the response to a particular input is desired, the computation is again very long because of the large number of coefficients and the repeated Laguerre and Hermite expansions.

3. It is desirable to be able to assign some meaning to the characterizing coefficients that would reveal some of the physically meaningful features of the system. This is extremely difficult under this formulation of the theory. The coefficients of the expansion are purely formal mathematical quantities and it appears futile to attempt to draw an analogy between them and physical properties of the system which they characterize.

4. A linear system which is characterized very simply by the classical linear theory is characterized very cumbersomely by this method. A vast number of coefficients is needed to identify a linear system. This is due to the fact that a very large number of Hermite functions is needed to represent a linear transformation.

5. It is very difficult to incorporate into Wiener's method any *a priori* information about the system so as to plan the computation for shorter lengths and reduce the number of the characterizing coefficients. Point (4) is an example of this serious shortcoming of this very general method: The method in being so very general fails to recognize a simple situation and treat it accordingly.

6. The derived nonlinear model is too cumbersome to use for prediction or comparison with experimental results even if a digital computer is available.

Later, Lee and Schetzen (1965) employed cross-correlation techniques and showed how the kernels $\{h_i\}$ can be directly evaluated utilizing the orthogonality properties of equations (8) and (10). Taking the average ($E\{\cdot\}$) of equation (8) we have

$$E\{y(t)\} = E\{h_0\} + E\{\int_0^\infty h_1(\tau)x(t-\tau)d\tau\} + E\{\iint_0^\infty h_2(\tau_1, \tau_2)x(t-\tau)x(t-\tau_2)d\tau_1 d\tau_2 - P\int_0^\infty h_2(\tau_2, \tau_2)d\tau_2\} + \ldots$$

and assuming stationarity of the system and the input we get

$$E\{y(t)\} = h_0,$$

recalling that $x(t)$ is a Gaussian white-noise signal of zero mean. Similarly, the first-order kernel can be obtained by taking

$$E[\{y(t) - G_0[h_0, x(t)]\}x(t-\sigma)] = E\{\sum_1^\infty G_n[h_n, x(t)]x(t-\sigma)\}.$$

Since $x(t-\sigma) = \int \delta(\tau-\sigma)x(t-\tau)d\tau$ is a functional of first degree, the functionals G_n, $n > 1$, are all orthogonal to it (Wiener, 1958). We therefore have

$$E\{y(t)x(t-\sigma)\} = \int_0^\infty h_1(\tau)E\{x(t-\tau)x(t-\sigma)\}d\tau = Ph_1(\sigma)$$

so that

$$h_1(\sigma) = \frac{1}{P}E\{y(t)x(t-\sigma)\}. \tag{11}$$

To get the second-order kernel we determine the higher order cross-correlation

$$E[\{y(t) - \sum_0^1 G_n[h_n, x(t)]\}x(t-\sigma_1)x(t-\sigma_2)]$$

and we proceed similarly, utilizing again the orthogonality of the Wiener series (cf., part II). The advantages of the orthogonality of the Wiener series are multiple:

(a) it allows measurement of the kernels to be made independently of each order, (b) it greatly alleviates the problem of signal contamination by noise sources at the input, output, or internally in the system, and (c) it allows a direct extension of the method to multi-input systems (Marmarelis and NaKa, 1974).

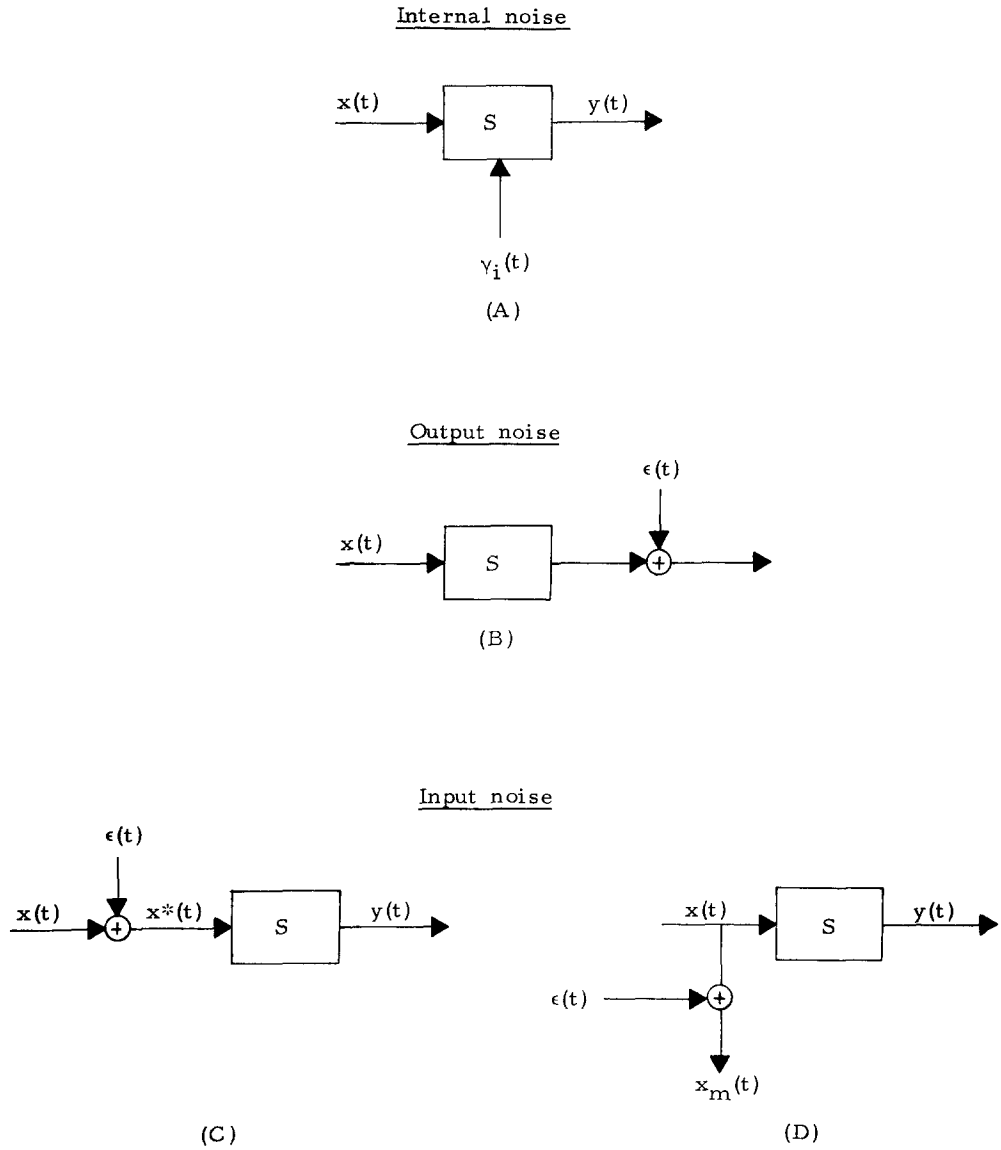

FIG. 2. Schematic showing sources of noise signals.

EXPERIMENTAL APPLICABILITY, SOURCES OF ERROR AND ACCURACY CALCULATIONS

The application of Wiener's method requires rather involved and lengthy digital computations. It is therefore useful to develop some criteria which would be indicative of how successful the approach might be when applied to structural systems, giving due consideration to the various assumptions underlying the technique.

Nonlinearities in structures strongly depend on the amplitude ranges and the frequency content of the input signals. Since we are interested in the earthquake response of

structures, it would be instructive to conduct tests with input amplitudes which are comparable to those created by close-in ground shaking. However, in the full scale testing of structures the generation of such large dynamic loads, which are white in character, may be very difficult. We are therefore forced to revert to naturally occurring loads that arise in the normal lifetime of structures. From the point of view of this analysis, we appear to have run into the following problem: While microtremors, created by random excitations of the ground in space and time, provide a very broad band spectrum, the amplitude levels are rather low; whereas strong ground shaking, while providing large amplitude inputs in a structure, would not be nearly as white in general due to various factors such as preferential frequency characteristics of the source function, the location of the observation point, and the filtering effect of the intervening region between the source and receiver, etc. It appears then that the effect of the nonwhite nature of the source would be an important consideration in the application of this technique to structural problems when earthquake excitations are used. This effect can be studied as follows:

Let $l(\tau)$ be the impulse response of a low-pass filter which transforms ideal white noise $x(t)$ to the real input "colored noise" signal $x^*(t)$. Then,

$$x^*(t) = \int_{-\infty}^{\infty} l(v)x(t-v)dv.$$

The first order kernel is estimated by taking the cross-correlation $\phi_{x^*y}(\tau)$ multiplied by a constant C_1 [$= 1/P$ if $x^*(t)$ is white noise, i.e., $\phi_{xx}(\tau) = P\delta(\tau)$] (see equation 11) and is given by

$$\hat{h}_1(\tau) = C_1\phi_{x^*y}(\tau) = C_1E\{y(t)x^*(t-\tau)\}$$

so that

$$\begin{aligned}\hat{h}_1(\tau) &= C_1\int_{-\infty}^{\infty} l(v)E\{y(t)x(t-\tau-v)\}dv \\ &= C_1\int_{-\infty}^{\infty} l(v)\phi_{xy}(\tau+v)dv = C_1\int_{-\infty}^{\infty} l(v)Ph_1(\tau+v)dv.\end{aligned}$$

Taking Fourier transforms of both sides

$$\hat{H}_1(\omega) = C_1P\bar{L}(\omega)H_1(\omega)$$

and

$$H_1(\omega) = \frac{\hat{H}_1(\omega)}{C_1P\bar{L}(\omega)} \tag{14}$$

where $L(\omega)$, $H_1(\omega)$, and $\hat{H}_1(\omega)$ are the Fourier transforms of $l(\tau)$, $h_1(\tau)$, and $\hat{h}_1(\tau)$ and $\bar{L}(\omega)$ is the complex conjugate of $L(\omega)$. From equation (14) it is noted that for $\hat{h}_1(\tau)$ to be a good estimate of $h_1(\tau)$, it is required that the bandwidth of input signal, $x^*(t)$, should completely cover the system bandwidth. For large frequencies ω the gain of the low pass filter $l(\tau)$ will be substantially different from 1 and therefore errors may arise in estimating $h_1(\tau)$ in this frequency range.

Hence, the input noise spectrum should be flat in character and should cover the complete frequency range in which the system's response is of interest. This provides the lower bound for the bandwidth of the input.

The records used in this analysis were low-pass filtered and sampled at 50 pts/sec, giving a Nyquist frequency of 25 Hz. The energy content in the earthquake signals beyond this frequency is generally quite small so that attention can be focused on determining the structural system characteristics in this frequency band range. Error contributions described by equation (14) would then be small if the spectrum is sufficiently flat in this range. The sampling rate chosen is commensurate with the band of frequencies in which

the energy is mainly concentrated and will therefore lead to only small aliasing errors. Also, if the system response shows an effective cutoff frequency, f_c, then the $\{h_i(\tau)\}$ can be completely ascertained by determining its value at $\Delta t = 1/2f_c$. If the estimation is done with a larger time spacing (assuming that the record length permits this), the higher frequency contents of the generalized impulse responses will be irretrievably lost. On the other hand, if the sampling rate is considerably smaller in attempting to measure the very high-frequency response, while keeping the number of samples a constant (because of computational considerations), the statistical variance of the cross-correlation estimates increases because the number of independent samples from which the cross-correlation is computed decreases.

The time length to which the kernels $\{h_i(\tau)\}$ must be computed depends on the memory, M, of the system. The memory, M, can be defined as that time t at which the response of the system to an impulse at time zero is negligibly small. Most structural systems exhibit the characteristics of lightly damped oscillators with the percentage of critical damping being at most about 7 to 10 per cent. This implies large settling times typically of the order of 5 to 20 sec. If the memory, M, is assumed too long, the number of computations required would be significantly increased in addition to the higher computer capacity required. On the other hand, if M is assumed to be too short, a systematic error will be introduced in the estimation process.

Finally, the temporal length of the excitation must be such as to give tolerable values of the variances of the different statistical averages that the cross-correlations represent. For the earthquake records, we are further limited in the choice of a utilizable record duration in that we need to choose segments of the record where the input-output can be considered stationary processes and where the system can be assumed to remain time-invariant. The length of record chosen then must be short enough so that the system is invariant during the identification interval, but is long enough as compared to the memory of the system so that the statistical estimates have tolerable variances. The assumption that the input-output process is a stationary one, although frequently used in earthquake engineering, is of course incorrect for earthquake records. For microtremor records, the situation is quite different. These low amplitude ground motions (of the order of $1 \sim 10$ microns or so) are so small that the structure behaves essentially in a linear fashion, indicating very little nonlinearity, a feature which we shall observe is quite significant during strong ground shaking. The input signal, however, is stationary in nature, its bandwidth far exceeding the bandwidth of interest of the system response. This larger bandwidth leads to considerable statistical variations in the computed cross-correlations. Assuming that the system is linear with its impulse response denoted by $h(\tau)$ (for the treatment of the nonlinear case see part II) and $x(t)$ is a Gaussian white input, the statistical variance of the estimate of $h_1(\tau)$ can be expressed as follows

$$\text{Var}\,\{\hat{h}_1(\tau)\} = A(R, M)\sigma_w{}^2$$

where, as discussed later, $A(R, M)$ is a function (< 1) of the record length, R, and system memory, M, and $\sigma_w{}^2$ is the variance of random variable $[y(t)x(t-\tau)]$ whose average, $E\{w\}$, is a direct measure of $h_1(\tau)$

$$\sigma_w{}^2 = E\{[x(t-\tau)\cdot\int h(v)x(t-v)\,dv]^2\} - \{E[x(t-\tau)\cdot\int h(v)x(t-v)\,dv]\}^2 \tag{15}$$

or

$$\sigma_w{}^2 = \iint h(v)h(\mu)E\{x(t-\tau)x(t-\tau)x(t-v)x(t-\mu)\}\,dv\,d\mu - \{\int h(v)E[x(t-\tau)x(t-v)]\,dv\}^2. \tag{16}$$

Considering that the average of the product of four Gaussian variables can be written as

$$\begin{aligned} E\{x(t-\tau)x(t-\tau)x(t-\nu)x(t-\mu)\} &= E\{x(t-\tau)x(t-\tau)\}\cdot E\{x(t-\nu)x(t-\mu)\} \\ &\quad + E\{x(t-\tau)x(t-\nu)\}\cdot E\{x(t-\tau)x(t-\mu)\} \\ &\quad + E\{x(t-\tau)x(t-\mu)\}\cdot E\{x(t-\tau)x(t-\nu)\} \end{aligned}$$

and the second term of (16) can be written as

$$\iint h(\nu)h(\mu)\cdot E\{x(t-\tau)x(t-\nu)\}\cdot E\{x(t-\tau)x(t-\mu)\}\,d\nu\,d\mu$$

equation (16) finally becomes

$$\sigma_w^2 = \text{var}\,(x)\int_{-\infty}^{\infty}\int h(\mu)h(\nu)\phi(\mu-\nu)\,d\mu\,d\nu + \left[\int h(\nu)\phi(\tau-\nu)\,d\nu\right]^2 \tag{17}$$

where

$$\phi(u) = \frac{\omega_0}{\pi}\cdot\frac{\sin(\omega_0 u)}{(\omega_0 u)} \tag{18}$$

is the autocorrelation of input noise $x(t)$, ω_0 is the bandwidth of this noise, and $\text{var}\,(x) = \phi(0)$ is the variance of the Gaussian input signal.

We consider the first term of equation (17). Writing $h(\nu)$ and $\phi(u)$ in terms of their Fourier transforms $H(\omega)$ and $\Phi(\omega)$ respectively, we obtain

$$\frac{\phi(0)}{4\pi^2}\int\int_{-\infty}^{\infty} H(\omega)\exp(-\omega\mu)\,d\omega\int_{-\infty}^{\infty} H(\omega')\Phi(\omega')\exp(-i\omega'\mu)\,d\omega'\,d\mu.$$

Noting that

$$\int_{-\infty}^{\infty} H(\omega)\exp(-i\omega\mu)\,d\omega = \int_{-\infty}^{\infty} H(-\omega)\exp(i\omega\mu)\,d\omega$$

and

$$H(-\omega) = H^*(\omega)$$

we finally obtain

$$\frac{\phi(0)}{4\pi^2}\int\int\int_{-\infty}^{\infty} H(\omega)H(\omega')\Phi(\omega')\exp[i(\omega-\omega')\mu]\,d\omega'\,d\omega\,d\mu.$$

Considering that

$$\int_{-\infty}^{\infty}\exp[i(\omega-\omega')\mu]\,d\mu = \delta(\omega-\omega')$$

and that $\Phi(\omega)$ is ideal low-pass with ω_0 bandwidth we finally get

$$\frac{\omega_0}{4\pi^3}\int_{-\omega_0}^{\omega_0}|H(\omega)|^2\,d\omega$$

which, indeed, is an increasing function of ω_0. Similarly, it can be shown that the second term can be written as

$$\frac{1}{4\pi^2}\left|\int_{-\omega_0}^{\omega_0} H(\omega)\exp(i\omega\tau)\,d\omega\right|^2.$$

Thus, we finally get for the variance of the estimated kernel,

$$\text{Var}\,[\hat{h}(\tau)] = A(R, M)\left[\frac{\omega_0}{4\pi^3}\int_{-\omega_0}^{\omega_0}|H(\omega)|^2\,d\omega + \frac{1}{4\pi^2}\left|\int_{-\omega_0}^{\omega_0} H(\omega)\exp(i\omega\tau)\,d\omega\right|^2\right] \tag{19}$$

where ω_0 is the bandwidth of the input signal and $H(\omega)$ is the Fourier transform of $h(t)$. We observe that Var $[\hat{h}(\tau)]$ generally increases with the bandwidth. However, the input signal, as previously mentioned, should at least cover the system bandwidth. Thus, the input noise bandwidth should be larger than the system bandwidth (as shown earlier) but

should not extend much beyond it. As discussed later, the variance of the kernel estimates also depends on the length of the characterizing experiment, and therefore the input band width and length of record both affect the kernel variance estimates.

Besides the errors which arise due to our assumptions in the model structure, errors due to the finiteness of the record analyzed and contaminating noise signals are important. For instance, the variance in $\hat{h}_1(\tau)$ due to the finite record length as obtained by the cross-correlation method would be

$$\text{Var}\{\hat{h}_1(\tau)\} = \frac{1}{N_i}\,\text{Var}\,[y(t)x(t-\tau)] = \frac{1}{N_i}\,\sigma_w{}^2$$

where N_i is the number of independent samples of $[y(t)x(t-\tau)]$ that can be obtained from the record. If M is the memory of the system and R is the record length, then

$$N_i \approx R/M.$$

Therefore, an estimate of the variance of $\hat{h}_1(\tau)$ is

$$\text{Var}\{\hat{h}_1(\tau)\} = (M/R)\sigma_w{}^2.$$

We note that for a given system, the rms error in the kernel estimates decreases proportionately to $\sqrt{R}$. For typical structures M is of the order of $1/\omega_n\xi$, where ω_n is the fundamental period (as obtained from linear analysis) and ξ is the percentage of critical damping. The record length R would then consist of N samples where $N = R/\Delta t$.

Most structures during low level (wind and microtremor) tests are subjected to distributed loads all along their height. However, their characterization through such experimentation is carried out by comparing the "input" signal at the base with the "output" signal at some level, ignoring the inputs to the structure at various other points (created, say, by the movement of people in the structure or the action of wind at various levels). These inputs, which actually may lead to considerable structural responses, are generally not considered in most of the experimental analyses. Insofar as the analysis attempts to characterize the structure without considering the effects of these multiple inputs that excite the system, one would need to consider these ignored inputs, γ_i, as noise inputs and then try to estimate the errors brought about by such "spurious" inputs in the estimation of the system kernels.

One can visualize these ignored inputs, γ_i, as following paths through the system which are different from the "input" path. The output $y(t)$, then, can be expressed as

$$y(t) = \sum_n \{G_n[h_n, x(t)]\} + \sum_i \sum_m \{H_m[k_{mi}, \gamma_i(t)]\} \tag{21}$$

assuming that the effect of these "disturbances" is simply additive to the system output. The more general case of nonlinear interaction between the inputs remains to be examined. For the linear case (see part II for the nonlinear case) we have $n = m = 1$. The estimation of the system kernel $h_1(\tau)$ through cross correlation gives

$$\begin{aligned}\phi_{xy}(\tau) &= E\{x(t-\tau)\int h_1(v)x(t-v)\,dv\} + E\{x(t-\tau)\sum_i \int K_{1i}(\mu)\gamma_i(t-\mu)\,d\mu\} \\ &= Ph_1(\tau) + \sum_i \int K_{1i}(\mu)\phi_{x\gamma i}(t-\mu)\,d\mu\end{aligned}$$

where the autocorrelation of white input $x(t)$ is $\phi_{xx}(\tau) = P\delta(\tau)$. Therefore, the estimated kernel $\hat{h}_1(\tau)$ is

$$\hat{h}_1(\tau) = h_1(\tau) + \left(\frac{1}{P}\right)\sum \int K_{1i}(\mu)\phi_{x\gamma_i}(t-\mu)\,d\mu.$$

If $\phi_{x\gamma_i}(\tau) = 0$, for all inputs γ_i, then $\hat{h}_1(\tau) = h_1(\tau)$ and the estimate of the system kernel is unadulterated by the contaminating noise signals $\gamma_i(t)$. This would be the case, for example, when $x(t)$ and $\gamma_i(t)$ are statistically independent, since in that case

$$\phi_{x\gamma_i}(\tau) = E\{x(t)\} \cdot E\{\gamma_i(t)\} = 0.$$

Errors created by output measurement noise $\varepsilon(t)$ (generally caused by digitization, transducer imperfections, and data processing) can also be studied in a similar manner.

Here we have,

$$\hat{h}_1(\tau) = \frac{1}{P}\phi_{yx}(\tau) = \frac{1}{P}E[\{\sum G_n[h_n, x(t)] + \varepsilon(t)\}x(t-\tau)]$$

$$= h_1(\tau) + \frac{1}{P}\phi_{x\varepsilon}(\tau).$$

If, for example, $x(t)$ and $\varepsilon(t)$ are independent, $\phi_{x\varepsilon}(\tau) = 0$ and then

$$\hat{h}_1(\tau) = h_1(\tau).$$

We notice that the estimation of the higher order ($n > 1$) nonlinear terms would involve $\phi_{xxxx\ldots x\varepsilon}(\tau_1, \tau_2, \ldots, \tau_n)$ so that the error would still be zero if, for example, x and ε are independent and $E[\varepsilon] = 0$, or n is odd. Thus, the contaminating noise does not affect the estimation of the characterizing kernel under rather general conditions, in particular when it is independent of the assumed input.

Errors, $\varepsilon(t)$, occurring at the input either as measurement errors or as deviations from a Gaussian signal, however, do tend to affect the kernel estimation. We distinguish here between two types of noise at the input: (1) Input noise which adulterates the Gaussian white-noise signal and goes through the system (as in case C of Figure 2), and (2) input measurement noise (as in case D of Figure 2). Proceeding similarly as above, it can be shown that

$$\hat{h}_1(\tau) = h_1(\tau) + \frac{1}{P}(E_1 + E_2 + E_3 + \ldots) \tag{22}$$

where $E_1, E_2, \ldots,$ are errors arising from $h_1, h_2, \ldots,$ respectively, and in case C are given by

$$E_1 = \int h_1(v)[\phi_{x\varepsilon}(\tau - v) + \phi_{\varepsilon x}(\tau - v) + \phi_{\varepsilon\varepsilon}(\tau - v)]dv \tag{23}$$

$$\begin{aligned} E_2 = \iint h_2(v_1, v_2)[&\phi_{xxx}(\tau - v_1, \tau - v_2) + \phi_{xx\varepsilon}(\tau - v_1, \tau - v_2) \\ &+ \phi_{x\varepsilon x}(\tau - v_1, \tau - v_2) + \phi_{x\varepsilon\varepsilon}(\tau - v_1, \tau - v_2) \\ &+ \phi_{\varepsilon xx}(\tau - v_1, \tau - v_2) + \phi_{\varepsilon x\varepsilon}(\tau - v_1, \tau - v_2) \\ &+ \phi_{\varepsilon\varepsilon x}(\tau - v_1, \tau - v_2) + \phi_{\varepsilon\varepsilon\varepsilon}(\tau - v_1, \tau - v_2)] \cdot dv_1 dv_2. \end{aligned} \tag{24}$$

In case D, the errors can be characterized as

$$E_1 = \int h_1(v)\phi_{x\varepsilon}(\tau - v)dv$$

$$E_2 = \int h_2(v_1, v_2)\phi_{xx\varepsilon}(\tau - v_1, \tau - v_2)dv_1 dv_2.$$

Note that, for example, $\phi_{x\varepsilon\varepsilon}(\tau_1, \tau_2) = \phi_{\varepsilon x\varepsilon}(-\tau_1, \tau_2 - \tau_1)$, and therefore only one of these ϕ's needs to be measured for any permutation of $(x, \varepsilon, \varepsilon)$. It is noted that the error terms increase with the order of nonlinearity of the system, and they are given as convolutions of signal-error correlations with the kernels. Therefore, input errors such as those of case C are more serious.

Let us consider one such input error that occurs quite commonly. This is the error

introduced by the truncation of the Gaussian amplitude distribution at very low and very high input signal levels. That is, the input signal is not an ideal Gaussian, but is defined by

$$P_r(x) = \frac{1}{\sqrt{2\pi}} \exp(-x^2/2) \qquad \text{if } |x| \leqq K.$$
$$= 0 \qquad \text{if } |x| > K.$$

Then, we have $x^*(t) = x(t) + \varepsilon(t)$ where $x(t)$ is ideally Gaussian and

$$\varepsilon(t) = \begin{cases} 0 & \text{if } |x(t)| < K \\ K - x(t) & \text{if } x(t) > K \\ -K - x(t) & \text{if } x(t) < -K. \end{cases}$$

From the formulas just derived, it is seen that the error depends on terms such as $\phi_{x\varepsilon}(\tau)$, $\phi_{\varepsilon\varepsilon}(\tau)$. Assuming $x(t)$ to be ideal white-noise (infinite bandwidth)

$$\phi_{x\varepsilon}(\tau) = C(K) \cdot \delta(\tau)$$

where

$$C(K) = \frac{2}{\sqrt{2\pi}} \int_K^\infty (Kx - x^2) \exp(-x^2/2) dx.$$

Further, in this case, it can be easily seen that $\phi_{x\varepsilon}(\tau) = \phi_{\varepsilon x}(\tau)$. Also,

$$\phi_{\varepsilon\varepsilon}(\tau) = D(K) \cdot \delta(\tau)$$

where

$$D(K) = \frac{2}{\sqrt{2\pi}} \int_K^\infty (K - x)^2 \exp(-x^2/2) dx.$$

Therefore (neglecting higher order kernels), the error $E(K)$ in the estimate of $h_1(\tau)$ can now be obtained by equation (22). Using the values of $\phi_{x\varepsilon}$ and $\phi_{\varepsilon\varepsilon}$ above, we get the estimate $\hat{h}_1(\tau)$ which is approximately given by

$$\hat{h}_1(\tau) \approx h_1(\tau)[1 + 2C(K) + D(K)]$$
$$\approx h_1(\tau)[1 + E(K)], \tag{25}$$

the exact equality holding if $h_n = 0$, $n > 1$ where

$$E(K) = \frac{2}{\sqrt{2\pi}} \int_K^\infty (K^2 - x^2) \exp(-x^2/2) dx.$$

Notice that the error function $E(K)$ is negative since $x^2 > K^2$ in $[K, \infty]$, i.e., we would tend to underestimate $h_1(\tau)$. This indicates that a small percentage error for $K > 2.5$ standard deviations of the Gaussian wave. It should be noted, however, that knowledge of the truncation level K can correct for this error simply by utilization of equation (25) where the value of K is determined for the given experiment.

Applications to a Reinforced Concrete Structure

In this section, the methods outlined above will be applied to earthquake accelerograms and ambient vibration test data obtained in a specific structure.

Description of the structure

The structure tested is the Robert Millikan Library at the campus of the California Institute of Technology. It is a nine-storey reinforced concrete building with one basement. Figure 3 shows the NS section, the typical floor plan and the overall dimensions. The structural system is characterized by two shear walls designed to withstand lateral loads in the NS direction, and a core wall which houses the elevator shaft and provides resistance to EW loads. Other structural details, phases of construction, and the properties of the underlying soil are described in detail by Kuroiwa (1967).

The choice of this building was dictated by the fact that it has been tested in numerous ways in the past. Both shaker and ambient tests have been carried out on it (Udwadia and Trifunac, 1972). Also, the records obtained during the San Fernando earthquake in California, 1971, are of exceptionally high quality.

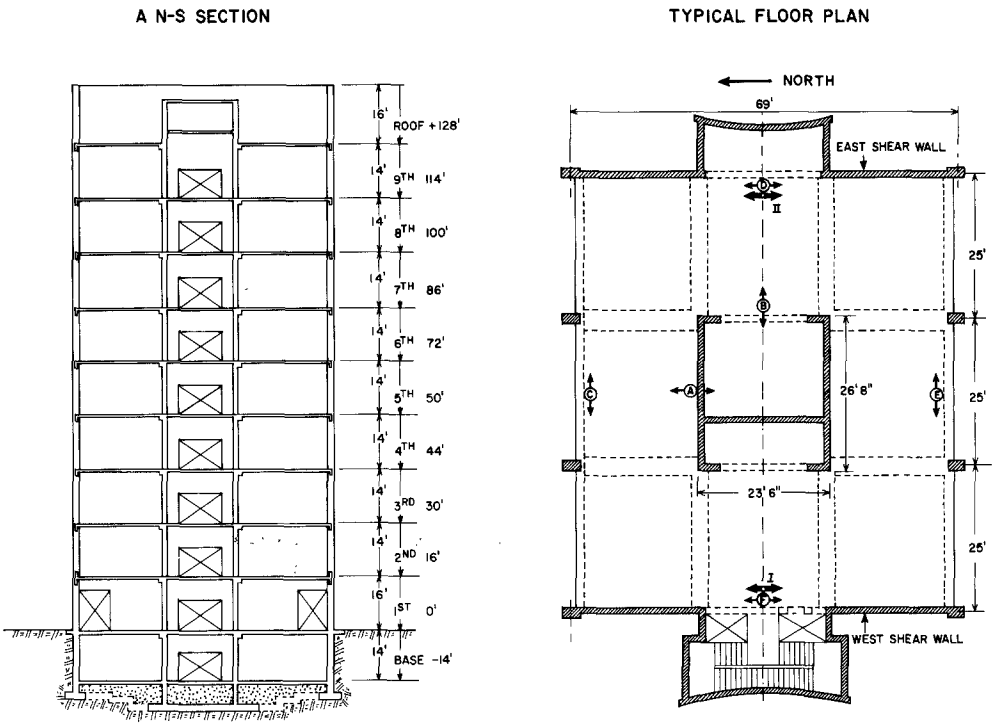

FIG. 3. Millikan Library Building. *Left*, a NS section; *right*, typical floor plan.

Records used for analysis

Both the NS and EW components of structural response have been studied. Records obtained during the 1971 San Fernando, California earthquake have been used (Figures 4 and 5). Also, the EW structural response to low-level amplitude motions was obtained by conducting an ambient vibration test in April 1973 when the small motions generated by wind and microtremors were recorded using sensitive vibration pickups (Figure 6). The actual experimental technique involved the placement of two Ranger seismometers (one in the basement and the other on the roof) whose outputs were amplified through a signal conditioner and recorded on analog magnetic tape. The tape was then converted to digital form on an analog-digital converter. The details of these tests have been extensively dealt with elsewhere (Udwadia and Trifunac, 1972) and will not be described here. The EW component of ground motion recorded during the earth-

quake is shown in Figure 4. The two sets of excitation cover a wide amplitude range and would be useful in studying the dependence of the structural characteristics on amplitude variations.

The record length to be used in the analysis, as stated before, must satisfy the following considerations: (a) the system properties must be invariant during the identification process, (b) its length must be appreciably larger than the system memory (to reduce the variance in the statistical estimates), and (c) it must constitute a stationary signal.

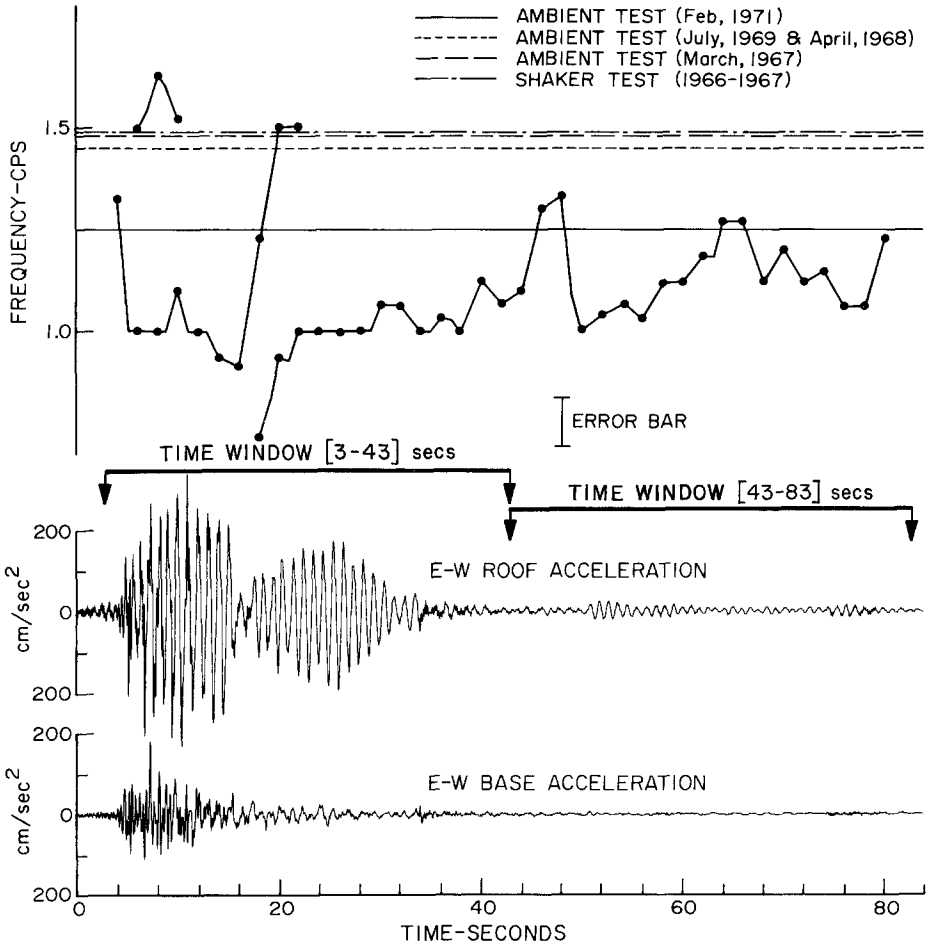

FIG. 4. EW accelerogram records showing the time windows chosen for analysis and the variation of the lowest EW translational frequency as obtained by moving window analysis taking a window length of 8 sec. Data are from the San Fernando earthquake of 1971 on the Millikan Library.

An idea of the duration of time during which the structure shows time-invariant characteristics can be obtained through a moving-window analysis of the earthquake record. The procedure for doing this is as follows: A time window of length T (8 sec in this case) is chosen. With the center of the time window located at $T/2$ sec, Fourier transforms of those portions of the input and output signals that lie within the time window are computed. The ratio of these transforms is computed giving the fundamental frequency, in an average sense, over that time interval. This gives one point on the frequency-time curve (Figures 4 and 5) whose time coordinate is the time corresponding to the center of the time window. The time window is next shifted along the time axis

a distance Δ (2 sec in this case); another average frequency is obtained and is plotted once more on the frequency-time curve. This approximate method is used to monitor frequency changes with time. Although the method suffers from several imperfections (e.g., the memory of the system, M, should be small compared with the length of the time window T), it gives a rough idea of the general zones in which the system can be considered time invariant.

From the frequency-time plots shown in Figures 4 and 5, two separate window lengths each of 40 sec duration have been chosen: one from 3 to 43 sec and the other from 43 to

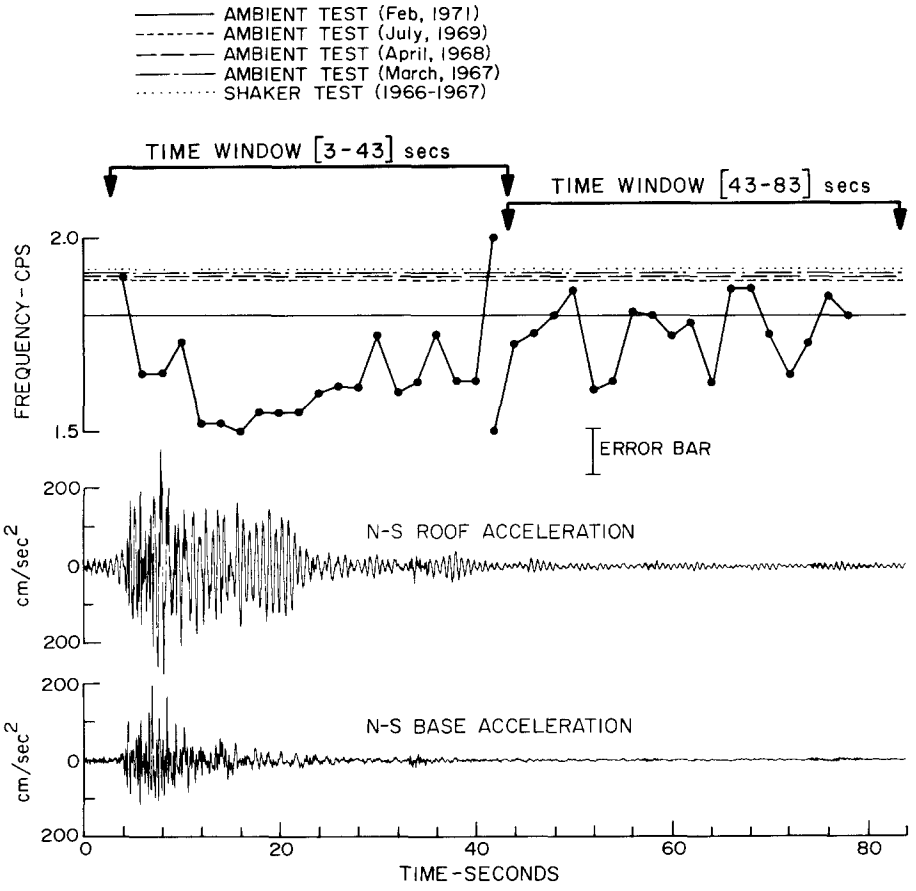

FIG. 5. NS accelerogram records showing the time windows chosen for analysis and the variations of the first and second NS translational frequency as obtained by moving window analysis taking a window length of 8 sec. Data are from the San Fernando earthquake of 1971 on the Millikan Library.

83 sec. The two zones also represent two different regimes of amplitude variations. These record lengths have adequate lengths when compared to correlation times $(1/\omega_n\xi)$ estimated from forced and man-excited tests.

The record length chosen for the ambient vibration test was 1 min. A typical segment of this record is shown in Figure 6. The record length needed would in general be longer in this case due to the wider power spectrum of these input ground motions, requiring longer lengths over which noise smoothing needs to be done.

Data processing

In the case of the earthquake records, standard Volume II data (obtained from the

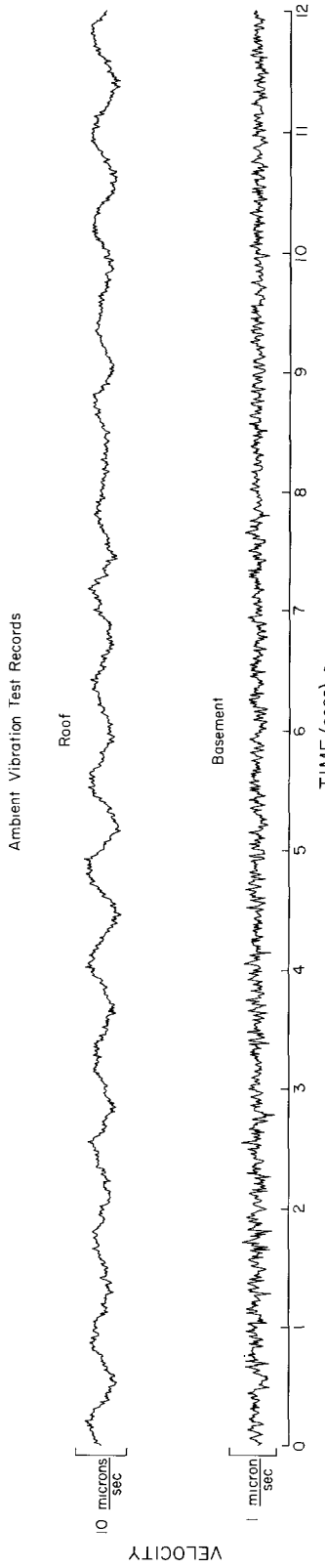

FIG. 6. A 10-sec segment of recorded motions at the basement and roof levels during an EW ambient vibration test.

Earthquake Engineering Laboratory at Caltech) were used. These data are obtained by low-pass filtering the recorded motions with a cutoff frequency of 25 Hz. The sampling rate is 50 pts/sec. The ambient test data was low-pass filtered with a cutoff frequency of 50 Hz and the sampling rate used was 100 pts/sec.

The power spectra of the input and output records were next computed. Based on the results of these calculations, the input data were multiplied by a constant factor in order to normalize the power level of the flat region of the input spectrum to unity. A similar scaling of the output spectrum was also done. This normalization was necessary to reduce the statistical variations in computing the first-order kernels. The power spectrum computations and the computations involved in determining the various cross-correlations were done using the Blackmann and Tukey (1958) algorithm to reduce the variance of the statistical estimates. For the power spectrum calculations this involved a splitting

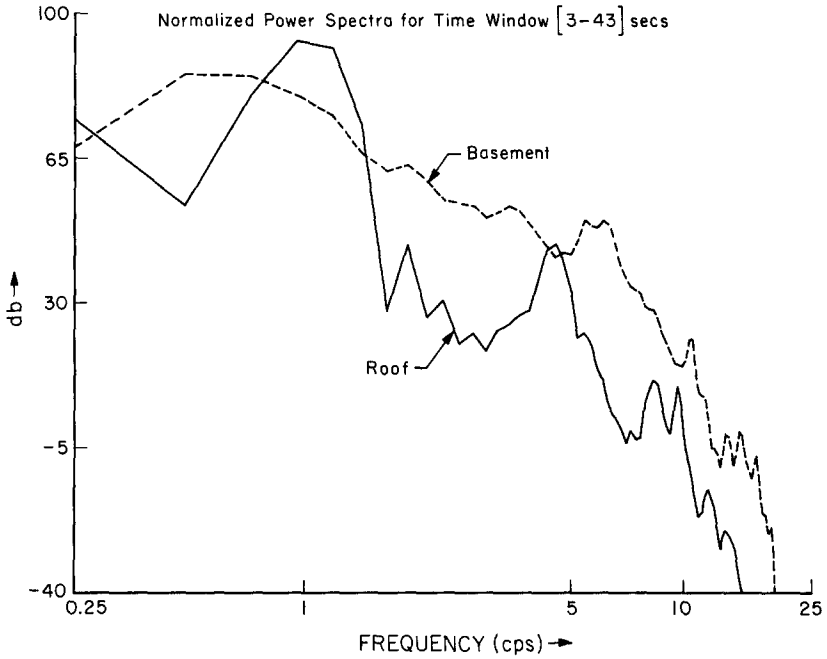

FIG. 7. Millikan Library. EW roof and basement records.

up of the record into three segments each of $N\Delta t/3$ duration, calculating the power spectrum for each of these, and then averaging them to give the final estimate. The normalized power spectra of the motions at the roof and the basement in the EW direction are indicated for the window lengths [3–43] and [43–83] sec in Figures 7 and 8. Similar computations were carried on the NS component of motion (cf., part II). We observe that both basement spectra are reasonable approximations to broad-band white processes. Typical, normalized frequency histograms are shown corresponding to the roof and basement records in Figure 9 for the time window [43–83] sec of the EW component. Dots representing points on a Gaussian curve are also plotted. Comparing the basement histogram with the Gaussian curve we observe the input to be Gaussian in character.

Figure 10 shows the normalized autocorrelation functions computed for the input signals represented by the two EW earthquake time windows and the ambient test data. These functions are symmetric about the zero lag point and therefore have been plotted

only for positive lags. The large "spike" at zero lag, indicated in curve C, shows that the ambient data provide a much better approximation to white noise than the earthquake data. By the same token, however, the presence of these higher frequencies in the ambient data would lead to higher statistical variances (see equation 14) so that longer records would be necessary (to perform adequate noise-smoothing). Curve B appears to have a periodic component having a period of about 1.3 sec, while curve A, although showing no such marked periodic feature, indicates an oscillatory behavior which dies out with time. The interpretation of these curves will be discussed in detail in the following section.

The first-order kernels computed, using the cross-correlation technique for the EW direction, have been shown in Figure 11. $h_1(\tau)$ corresponds to the time window [3–43] sec, $k_1(\tau)$ to the time window [43–83] sec, and $l_1(\tau)$ to the ambient vibration test. We observe that there is a marked difference in the nature of the functions. While the $h_1(\tau)$ kernel

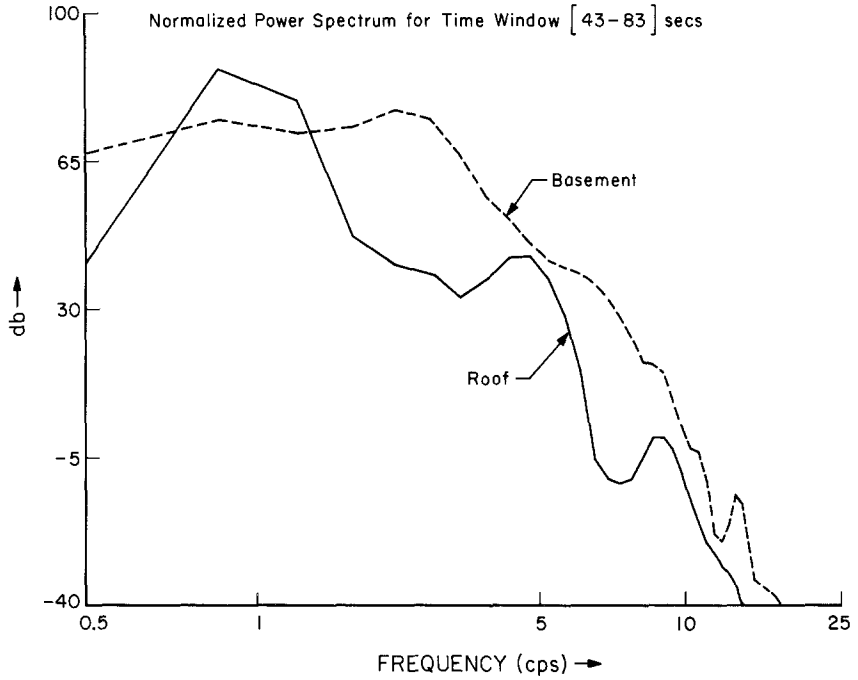

FIG. 8. Millikan Library. EW roof and basement records.

starts out with larger amplitudes (in its first cycle), it decays rapidly. The $k_1(\tau)$ and $l_1(\tau)$ kernels, in comparison, begin with successively smaller amplitudes and decay much more gradually. Interpreting these functions as being the impulse responses, the mean period changes from 0.98 sec for $h_1(\tau)$, to 0.9 sec for $k_1(\tau)$, and to 0.78 sec for $l_1(\tau)$. Considering these responses to be physically interpretable in terms of the viscously damped oscillator, estimates of the values of ξ range from about 5.5 per cent for $h_1(\tau)$, 3.5 per cent for $k_1(\tau)$, and 1.3 per cent for $l_1(\tau)$. The functions h_1, k_1, and l_1 have not been smoothed in any way and are results of the direct computations. The higher-frequency component in the $l_1(\tau)$ kernel is caused by the fact that the input is broader in its frequency characteristics, the relative proportion of the higher-frequency contents being more than in the earthquake data (see Figure 10). This higher proportion, although it allows the building to be tested at higher frequencies, increases the statistical variance of the kernel estimates as observed earlier. The $l_1(\tau)$ kernel was computed out to 20 sec. However, for comparison purposes only, the first 10 sec have been shown in Figure 11.

Having estimated the first-order kernels (i.e., the best linear model of the system, in the mean-square sense), the response of the model to the same input ground motions was determined, and a comparison with the measured response made, so as to provide a test

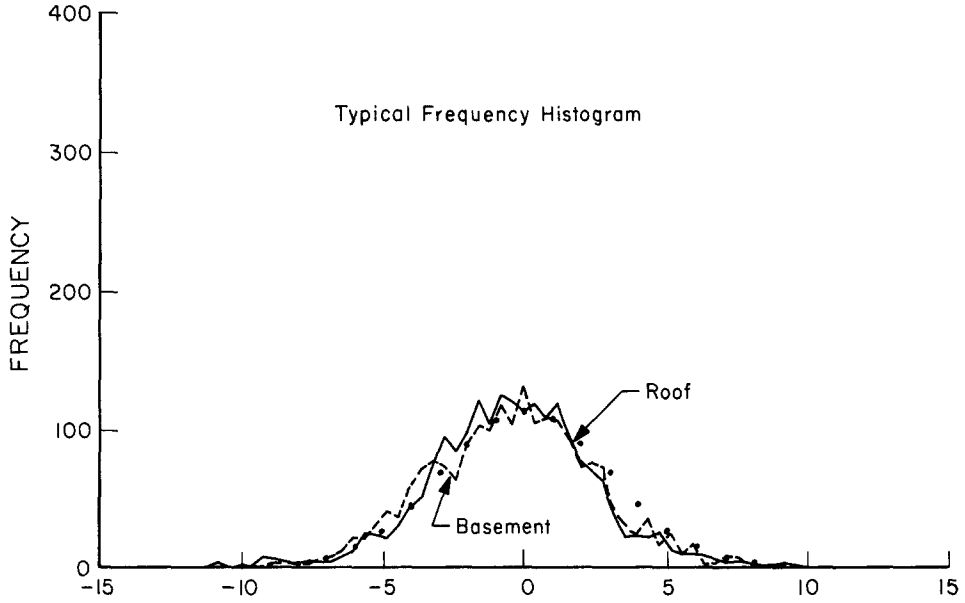

FIG. 9. Typical frequency histogram of ground motions. Dots indicate a Gaussian curve.

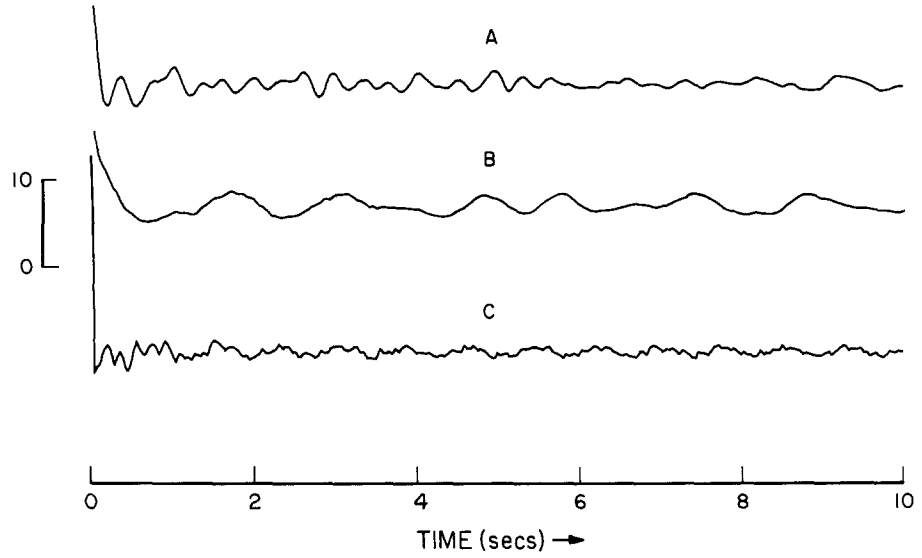

FIG. 10. Normalized autocorrelation functions for input signals used in studying EW response. (A) Time window [3–43] sec, (B) time window [43–83] sec, (C) ambient vibration test.

for the validity of the model. The response for the first 10 sec of ground motion was calculated for the EW motion corresponding to the [3–43]-sec window. This comparison is shown in Figure 12. The model response indicated agrees well with the observed

response, although the model appears to be predicting slightly lower amplitudes than those actually recorded. Also significantly missing from the model response are the higher-frequency ripples which are dominant in the measured response. The model response indicates the presence of sharper peaks, the peaks in the measured response being broader in nature.

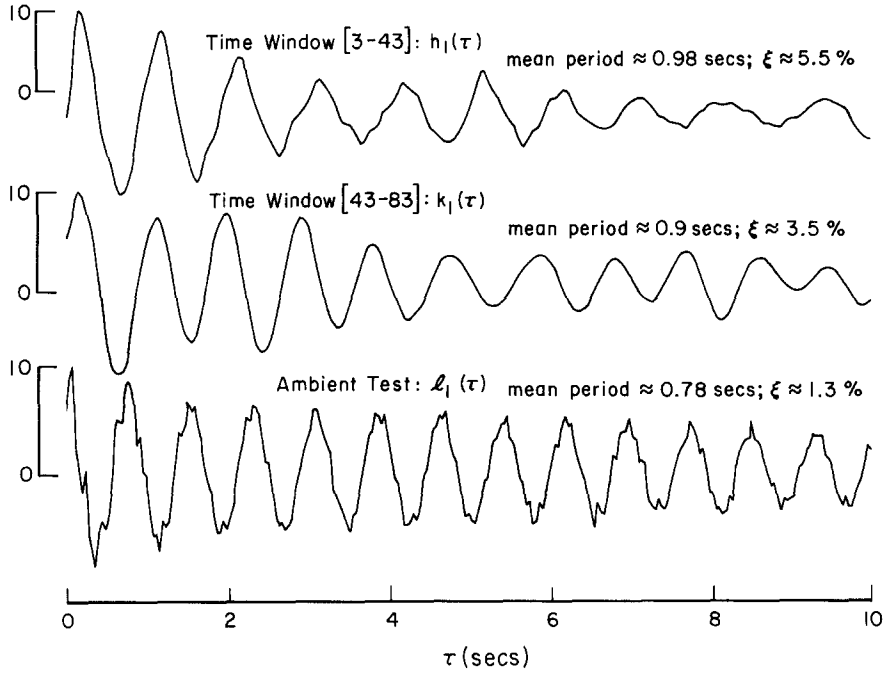

FIG. 11. Millikan Building Response: $h_1(\tau)$, $k_1(\tau)$, and $l_1(\tau)$. The computed first-order kernels for the EW direction which correspond to the time window [3–43] sec, the time window [43–83] sec, and a 1-min length of ambient data, respectively.

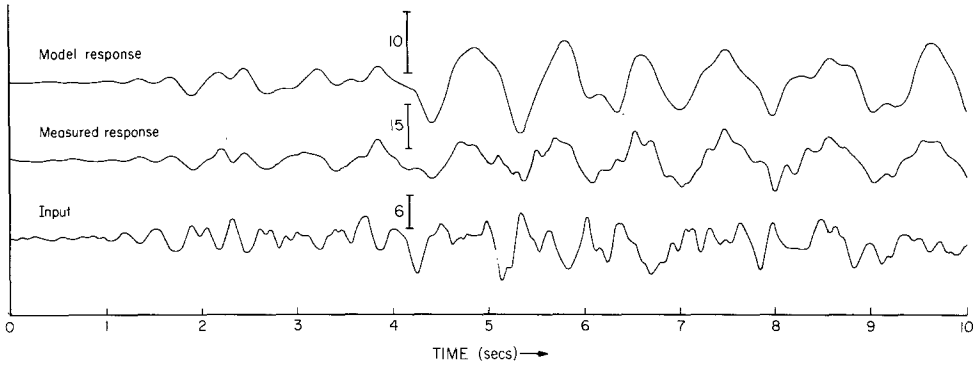

FIG. 12. Millikan Library. This figure shows a comparison between the observed EW ground motions at the roof and those computed using a linear model of the system.

Model responses for the [43–83] EW window as for the NS direction together with the spectra of the measured responses, the linear model responses, and the nonlinear model responses will be deferred until the second part of this study. Many of the discrepancies between the linear model response and the measured response will be resolved to a large extent when the corresponding nonlinear kernels of the system are computed and their contribution to the total response is determined. This is done in part II of this study.

For example, the second-order kernel $h_2(\tau_1, \tau_2)$ and its associated integral

$$\iint h_2(\tau_1, \tau_2)x(t-\tau_1)x(t-\tau_2)d\tau_1 d\tau_2$$

measure naturally the second harmonic nonlinear response and will therefore account for some of the high-frequency ripples present in the measured response but not exhibited by the linear model response.

Discussion

The purpose of this paper was to develop and evaluate a suitable nonlinear identification method for studying the dynamics of structural systems. The technique has been shown to be simple and the results obtained, so far, quite encouraging. The method allows a simple visualization of the dynamic system in terms of a linear element and nonlinear elements, so that the relative extent of the linear and nonlinear contributions to the total response can be studied.

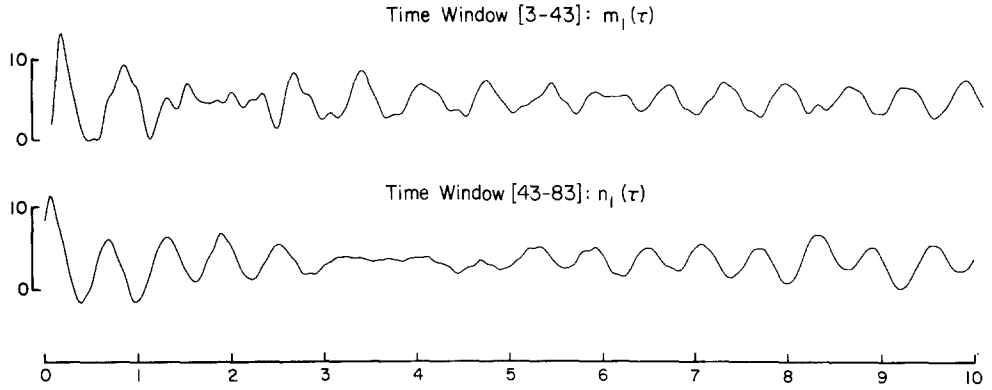

FIG. 13. Millikan Building Response: $m_1(\tau)$ and $n_1(\tau)$. The computed first-order kernels for the NS direction which correspond to the time windows [3–43] sec and [43–83] sec, respectively.

However, the method utilized leads to some difficulties in terms of computer time and storage. The computation time increases approximately exponentially with the order of the kernel, whereas the higher-order kernels seem to require very large computer storage. While the second problem can be easily tackled through the use of virtual machine memory, the first one seems to be rather difficult to circumvent using the current algorithms. The use of multidimensional Fast Fourier transforms in computing the higher-order correlations is being currently investigated. This would not only drastically reduce computation costs, but it would make it possible to process the data in real time.

Of a slightly more fundamental nature is the assumption of a white-noise input. To illustrate this point, the first-order kernels for the NS direction were computed for both time windows ([3–43] and [43–83] sec) and have been displayed in Figure 13. The two kernels denoted as $m_1(\tau)$ and $n_1(\tau)$ (corresponding to the time windows [3–43] and [43–83], respectively) show contamination by a lower frequency component. This has been attributed to the nonwhite nature of the input signal which appears to have a considerable concentration of energy around 0.75 Hz. These figures illustrate the limitations of the white-noise approach, indicating a necessary improvement or extension of the technique (cf., part II). The Fourier transform approach appears to be more advantageous here, although it suffers from other problems such as high-frequency noise.

Consider, for instance, the linear system

$$y(t) = \int_0^\infty h(t)x(t-\tau)d\tau.$$

Taking transforms on either side of the equation, we have

$$\tilde{Y}(\omega) = \tilde{H}(\omega)\tilde{X}(\omega)$$

where $\tilde{Y}$, $\tilde{H}$, and $\tilde{X}$ are the transforms of $y(t)$, $h(t)$, and $x(t)$ and,

$$|H(\omega)| = \frac{|\tilde{Y}(\omega)|}{|\tilde{X}(\omega)|}.$$

Assuming the acceleration spectrum of the earthquake to have the form

$$|\tilde{X}(\omega)| = \frac{\alpha^2}{\alpha^2+\omega^2}$$

a small perturbation $\delta y(t)$ in the output whose Fourier transform is

$$\begin{aligned} \delta_N \tilde{Y}(\omega) &= \frac{1}{N} && N < \omega < N+1 \\ &= 0 && \text{otherwise} \end{aligned}$$

would lead to a perturbation $\delta\tilde{H}(\omega)$ in the determination of the kernel, given by

$$|\delta\tilde{H}(\omega)| = \frac{\alpha^2+\omega^2}{\alpha^2}\,\delta_N \tilde{Y}(\omega).$$

We then have the problem, that although the noise

$$\begin{aligned} |\delta_N y| = |\delta\,\tilde{Y}(\omega)| &\to 0 \quad \text{as} \quad N \to \infty, \\ |\delta\tilde{H}(\omega)| &\to \infty \quad \text{as} \quad N \to \infty. \end{aligned}$$

The problem is ill posed, and large inaccuracies would arise in the determination of $\tilde{H}(\omega)$ if we went to high frequencies—a situation described as high-frequency noise. Furthermore, unlike the cross-correlation technique, this method is extremely sensitive to noise perturbations in both the input and output records as well as noise perturbations created by ignored inputs as discussed earlier.

The linear kernels (Figures 10 and 12) computed show some interesting features in that they do not appear to be zero at $\tau = 0$ as would be expected for a causal physical system with finite speeds of signal propagation. This may be a consequence of the unknown initial conditions of the system which is being studied, together with its very low damping (resulting in a long memory). This problem would have persisted, it may be noted, even if the accelerograph record analyzed had started from zero time, for the structure would have been already vibrating when the accelerograph was triggered. However, the main factor which appears to cause such a displacement of the h_1 function is the presence of feedback.

The feedback model (Figure 1) which was described shows that the output of system between the node points p and r is fed back through the element A back to the input. To clarify this effect let us consider A to be unity (i.e., the output at r is fed back directly, although possibly with a time delay, into node p). Then the output at time $(t-t_d)$ where t_d will take into account the time delays in the system, will be fed back into the input at time t, so that $\overline{x(t)y(t-t_d)}$ is not zero for all positive values of t_d, because $x(t)$ would be

composed, in part, of $y(t-t_d)$. The extent of this feedback effect would depend on the level of the output at r as compared with the input and the nature of modification the signal undergoes as it passes through the element A (Figure 1b).

An interesting aspect which emerges from this model is that even if the true input (i_t) were white in the open-loop case, the feedback which causes the output of the filter elements to be mixed with the white input prevents it from being white. However, as pointed out earlier, so long as the input spectrum is sufficiently flat (equation 13), this does not pose a serious problem to the applicability of the general theory. Also, the fact that the kernel estimation is insensitive to contaminating noises, as was shown by the earlier analysis in the section on experimental applicability, makes the general technique quite efficacious.

Conclusions

Wiener's general theory of nonlinear system identification has been applied to the dynamic identification of a structural system from input-output data obtained during an earthquake and during an ambient vibration test. Before the method could be applied, the general zones where the system remained time-invariant were determined using a moving-window analysis technique. It was found that the method is practically applicable to structural systems provided certain minimum conditions exist. These can be ascertained through certain preliminary considerations and analyses. These include such items as (a) a rough knowledge of the system memory to determine the extent to which the kernels should be estimated, (b) estimation of the required length of the test for a certain accuracy, (c) choice of the bandwidth of the input excitation, and others. In addition, the effect of contaminating noise signals upon the kernel estimates is considered, and it is shown that the cross-correlation techniques used greatly reduce these unwanted effects. It was found that computer storage and time are two critically important factors to be considered. In this part of the study (part I) only the linear Wiener-Kernel model was estimated out to 10 sec for the earthquake data and up to 20 sec for the ambient data.

The studies indicate that the kernels computed for the two different time windows and the ambient EW experiment are quite different from each other in their frequency content, their equivalent damping ratios and their general amplitude levels. The building's first-order kernel showed time varying characteristics. The variations in time (although possibly caused in part by the fact that the ambient test was a low-level test) seem to indicate, in concurrence with previous investigations (Udwadia and Trifunac, 1975), the presence of a gradual "healing" process after the strong shaking caused by the San Fernando event.

The building response to the earthquake excitation in the EW direction was computed using the estimated linear kernels (cf., part II) and it was compared with the measured building response. It was found that the two responses were quite close but that some discrepancies existed. These discrepancies will be partly resolved by the introduction of the higher-order nonlinearities in the model, thereby providing a better system characterization, in part II.

Acknowledgments

We thank Professors G. W. Housner, D. E. Hudson, P. C. Jennings, and M. D. Trifunac for critical reading of the manuscript and some valuable remarks. Thanks are also due to Professor G. D. McCann for the use of his computer facility during the initial phases of this research.

This work was supported by grants from the National Science Foundation and the Earthquake Research Affiliates Program of the California Institute of Technology.

REFERENCES

Blackman and Tukey (1958). *The Measurement of Power Spectra*, Dover, New York.

Brilliant, M. B. (1958). Theory of the Analysis of Nonlinear Systems, *Tech. Rept. 345*, Research Lab. of Electronics, Mass. Inst. Tech., Cambridge, Mass.

Bose, A. G. (1956). A Theory of Nonlinear Systems, *Tech. Rept. 309*, Research Lab of Electronics, Mass. Inst. Tech., Cambridge, Mass.

Gersch, W., N. Nielsen, and H. Akaibe (1972). Maximum likelihood estimation of structural parameters from random vibration data, *Proc. World Conf. Earthquake Eng., 5th, Rome.*

Iemura, H. and P. C. Jennings (1973). Hysteric response of a nine-story building during the San Fernando earthquake, Earthquake Engineering Research Laboratory, California Institute of Technology, Pasadena.

Kuroiwa, J. (1967). Vibration test of a multistory building, Earthquake Engineering Research Laboratory, California Institute of Technology, Pasadena.

Lee, Y. W. and M. Schetzen (1965). Measurement of the kernels of a nonlinear system by cross correlation, *Intern. J. Control* **2**, 237–254.

Marmarelis, P. Z. and K.-I. Naka (1973). Nonlinear analysis and synthesis of receptive-field responses in the catfish retina. I. Horizontal cell-ganglion cell chain, *J. Neurophysiol.* **36**, 619–633.

Marmarelis, P. Z. and K.-I. Naka (1974). Identification of multi-input biological systems, *IEEE Trans. Biomedical Engineering* **21**, 88–101.

Marmarelis, P. and F. Udwadia (1976). Identification of building structural systems. Part II. The nonlinear case, *Bull. Seism. Soc. Am.* **66**, 153–171.

Nielsen, N. N. (1966). Vibration tests on a nine-story steel frame building, *J. Eng. Mech. Div., A.S.C.E.* **92**, 82–110.

Udwadia, F. E. and M. D. Trifunac (1972). Ambient vibration tests of full scale structures, *Proc. World Conf. Earthquake Eng., 5th, Rome.*

Udwadia, F. E. and M. D. Trifunac (1975). Time and amplitude dependent response of structures, submitted for publication.

Wiener, N. (1958). Nonlinear problems in random theory, Mass. Inst. Tech., Cambridge, Mass.

CALIFORNIA INSTITUTE OF TECHNOLOGY
PASADENA, CALIFORNIA 97109

Manuscript received February 5, 1975